Suspended particle dynamics in a southern California urban estuary during the dry season

Drew Ackerman and Nikolay P. Nezlin

Abstract

Sediments in urbanized estuaries often have elevated levels of pollutants and are the subject of cleanup or management actions. Understanding particle dynamics in an estuary can provide insight into possible sediment sources and can inform management decisions. This study deployed a laser scatterometer (LISST-100X, Sequoia Scientific, Inc., Bellevue, WA) in the Ballona Creek Estuary (BCE), in southern California, throughout the summer of 2008 to investigate particle dynamics. The LISST-100X sampled total suspended material (TSM) in the near-sediment water column analyzed particle size frequency in 32 log-spaced diameters between 2.73 and 462 µm once every 6 minutes. Tidal elevation was measured at the site to estimate the tidal prism throughout the deployment. The bio-fouling observed between instrument servicing was approximated by logistic equation and removed from the raw data. The detrended data matrix on particle size distribution was transformed using Principal Component Analysis (PCA) multivariate statistics. The three leading PCA modes (>92% of total variability) were attributed to different particle size classes: mid-size (71%), small-size (14%), and large-size (7%). Domination of mid-size TSM was associated with high phytoplankton biomass in the coastal waters. This conclusion was based on correlation between the first PCA mode and remotely-sensed satellite (MODIS-Aqua) observations of surface chlorophyll a (CHL) concentrations in Santa Monica Bay. In addition, first PCA mode variability was mostly diurnal rather than semidiurnal (i.e., associated with phytoplankton growth rather than tidal transport). Small- and large-size sediments (second and third PCA modes) were dominated by semi-diurnal variability, indicating the role of tidal circulation in forcing horizontal transport and resuspension. The relationship between tides and small- and large-particle TSM was non-linear, indicating high spatial heterogeneity of these particles. The extremes of both small and large-particle TSM were observed during spring ebb tides when low concentrations of small-size particles and high concentrations of large-size particles were transported down-estuary. The results from this monitoring indicate that greatest pollutant level reductions in the BCE would come from minimizing the pollutant concentrations on sediment input into the system rather than efforts to clean up sediments *in situ*.

Introduction

Urban estuaries frequently have elevated sediment pollutant levels due to runoff from the surrounding watersheds. Ashley and Napier (2005) found elevated trace metal concentrations in sediments for an urban estuary in north coastal New South Wales, Australia where there was evidence of copper, zinc, iron, and aluminum mobility. On the west coast of the United States, elevated metals concentrations in California have been observed in the San Francisco and Tijuana estuaries, as well as San Diego Bay (Fairey *et al*. 1998, Hornberger *et al*. 1999, O'Day *et al*. 2000). In the eastern United States, polycyclic aromatic hydrocarbon (PAH) concentrations decreased in the Potomac and Shenandoah River estuaries sediments with distance from urban centers and were correlated with population densities in surrounding drainage areas (Foster and Cui 2008).

Elevated pollutant levels in estuarine sediments have been extensively documented to have adverse biologic impacts. Anderson *et al*. (2007) demonstrated that elevated pollutant levels from urban inputs into the San Francisco estuary caused adverse toxicity in bivalve embryos. Also, elevated metals have been shown to reduce benthic biodiversity (Mucha *et al*. 2003). Bollmohr *et al*. (2009) observed impacts on benthic communities from exposure to endosulfan and chlorpyrifos in an intermittently open estuary in the Lourens River (South Africa). These impacts frequently result in management requirements for mitigation.

Before developing a management strategy, it is necessary to accurately characterize particle behavior. For example, if particles are relatively immobile, dredging and removal would be an appropriate management approach. Conversely, mobile contaminated sediments would be best managed through source control. A better understanding of how differently-sized sediments respond under different forcing conditions is essential to any management plan. For example, copper concentrations in an urban western Australia estuary were shown to increase with increases in clay content, as particulates were relatively immobile (Rate *et al*. 2000). Higher metals concentrations were found to be preferably bound to fine particles, such as silicates, oxides, and hydroxides of silicon, iron, and aluminum (Liu *et al*. 2004). Principal component analysis also showed that finer grain sizes had higher metals and organic matter concentrations in the Kastela Bay in Adriatic waters (Ujevic *et al*. 2000). Bacterial contamination (total coliforms and *Escherichia coli*) was associated with small-size particles (3.2 - 4.5 µm) in a medium-sized Australian reservoir (Hipsey *et al*. 2006).

Deploying an instrument that can continuously monitor suspended particle concentrations offers an opportunity to characterize suspended particle behavior in an urban estuary. Ballona Creek is an example of a heavily urbanized estuary in southern California; the estuary has historically elevated levels of contaminants in the water and sediment. Ballona Creek estuary (BCE) sediments have elevated PAH levels (Sabin *et al*. 2008), metals (Buffleben *et al*. 2002), and toxicity impacts (Bay *et al*. 1998). Because of these impacts, the estuary has been placed on the EPA 303(d) list of contaminated waterbodies. Thus, a management plan to mitigate those pollutants is required.

The purpose of this study was to use a novel technology to continually monitor total suspended material in the BCE and to characterize those particles using multivariate statistics. Sampling was conducted during summer 2008 when there were no significant terrestrial sediment loadings. The summer months allow for better investigation of accumulated sediment because terrestrial inputs into the BCE are relatively minor compared to wet weather loads.

Ballona Creek Estuary

The BCE is located in Los Angeles, California. Its watershed drains 335 km^2 of area that is nearly 85% developed. The estuary is confined and trapezoidal with rip-rap sides; it is approximately 100 m wide and 3 m deep at the seaward boundary at mean water level. The estuary is located south of the Marina del Rey marina and protected to the west (seaward) by a breakwater (Figure 1). Dry weather flows into BCE are typically less than 1 $m^3\ s^{-1}$, with total suspended sediment concentrations typically ~20 $mg\ L^{-1}$ (Stein and Tiefenthaler 2005). The dry weather inputs into the BCE average 37% of the total annual volume and 9% of the sediment load (Stein and Ackerman 2007).

Methods

The TSM concentrations were monitored in the BCE during the summer of 2008 using a laser refractometer. That data was log-transformed and detrended to remove bio-fouling effects. Principal component analysis was performed on the transformed data. The three most significant PCA modes were identified and relationships between particle size, mode, tides, and CHL concentrations investigated.

TSM Data Collection

The TSM concentrations of different size classes were measured using a LISST-100X Laser In-Situ Scattering and Transmissometry (LISST; Sequoia Scientific, Inc., Bellevue, WA). The LISST uses laser refractometry to measure volumetric concentrations (in microliters per liter) for particles in 32 size classes based on log-spaced diameters ranging from 2.72 to 462 µm. Particle sizes were inferred based on the amount of scattered laser light that particles induced when the laser was shined through a known parcel of water (Sequoia Scientific 2007). Previous calibration experiments showed that LISST provides fast and accurate measurements of suspended sediment concentrations adequately representing the volumetric size distribution of different types of suspended particles, including inorganic sediments, phytoplankton, and bacterial aggregates (Traykovski *et al*. 1999, Gartner *et al*. 2001, Mikkelsen and Pejrup 2001, Serra *et al*. 2001, Slade and Boss 2006, Styles 2006, Meral 2008).

The LISST was deployed near the mouth of the BCE from May 29 to August 27, 2008. The instrument was housed in a 20-cm pipe, which was mounted to a platform resting on the bottom and oriented cross channel. The instrument window was approximately 10 cm above the channel bottom sediment surface. Samples were collected by averaging 10

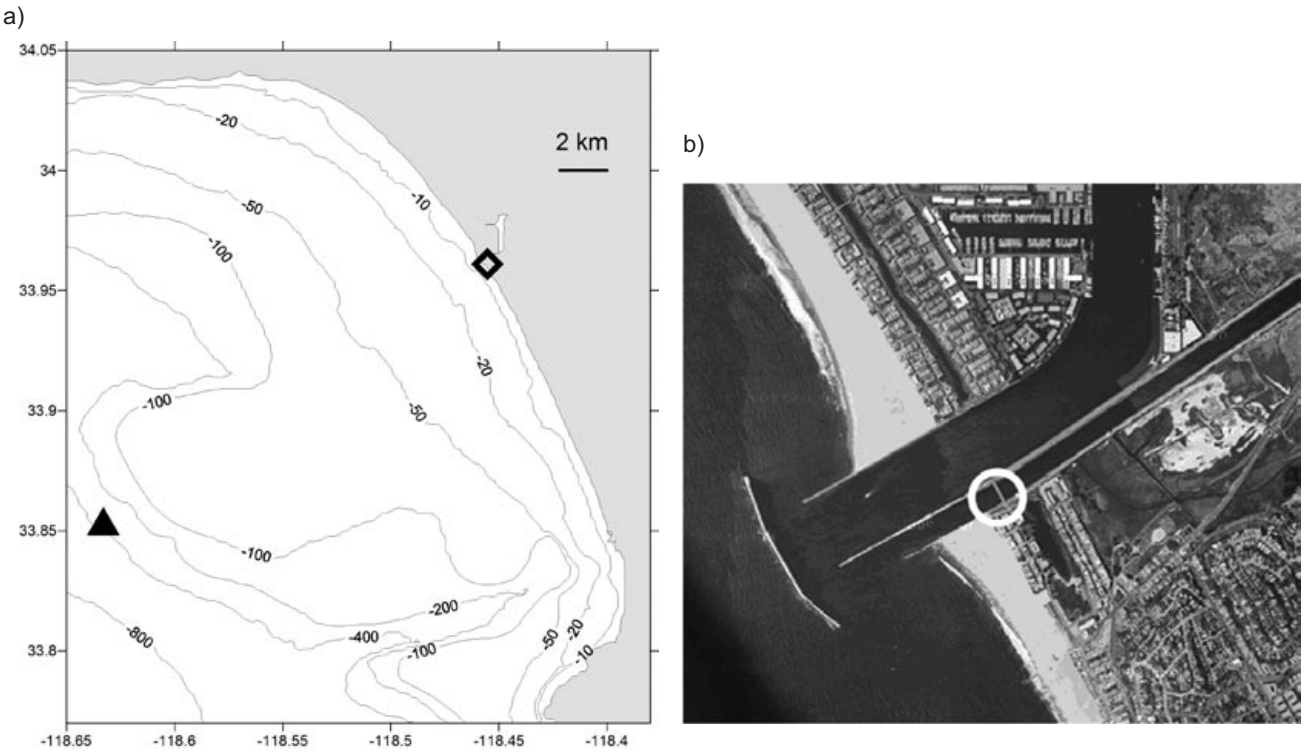

Figure 1. Location of the LISST-100X (diamond) in the Ballona Creek Estuary and the NDBC buoy 46221 (triangle) in the Santa Monica Bay (a); Location of the LISST-100X (white circle) within the Ballona Creek Estuary (b).

laser bursts every 6 minutes. Maintenance was performed weekly to bi-weekly with data downloaded and the instrument optics cleaned and calibrated according to manufacture specifications (Sequoia Scientific 2007). Twenty-one days of data were lost due to deployment difficulties and because the instrument was turned off during redeployment. Overall, usable particle size data was present for 73% of the total deployment.

A HOBO U20-001-01 pressure transducer (HOBO; Onset Computer Corporation, Bourne, MA) was co-deployed with the LISST to measure pressure and temperature throughout the sampling period. HOBO data was downloaded concurrently with the LISST data. Atmospheric pressure data from the Los Angeles International Airport (www.ncdc.gov) was subtracted from measured pressure data to obtain water column depths. Because the transducer was not on a permanent platform, it was in a slightly different location for each deployment. Mean depth recorded by the HOBO during each deployment period was subtracted from the water-depth time series to determine tidal stage.

Wave conditions and water temperature in Santa Monica Bay (SMB) were characterized by a stationary buoy 46221 (33°51'16" N; 118°37'59" W; water depth: 365 m) 20 km southwest of the BCE mouth (Figure 1a). Measurements of significant wave height and surface water temperature were obtained from the National Data Buoy Center (NDBC; www.ndbc.noaa.gov).

Phytoplankton biomass assessments in the SMB were derived from the remotely-sensed satellite measurements of ocean color collected by a Moderate Resolution Imaging Spectroradiometer (MODIS) on the Aqua satellite platform. The Level 3 Standard Mapped Images (SMI; reprocessing 5.2) of surface CHL concentration were obtained from National Aeronautics and Space Administration Goddard Space Flight Center Distributed Active Archive Center (NASA GSFC DAAC; Acker *et al*. 2002). The Level 3 SMI format is a regular grid of equidistant cylindrical projections with 360º/8192 pixels (~4.5-km resolution). The basic algorithm used at the GSFC for calculating CHL was described by O'Reilly *et al*. (1998). The CHL measurements in the SMB (33.77ºN–34.05ºN; 118.65ºW–118.38ºW) collected during May-August 2008 were extracted from global grids and averaged as medians for each day. Medians rather than arithmetic means were used because statistical distribution of remotely-sensed chlorophyll is typically lognormal rather than

normal (Banse and English 1994, Campbell 1995); medians are closer to modal values regardless of statistical distribution.

Sample Processing

Percent optical transmission was used to ensure that data of sufficient quality was used in the analyses. Observations with less than 20% optical transmission were discarded as erroneous readings as per manufacture recommendation (Sequoia Science, personal communication). The TSM for each size class was log-transformed before processing with zero value substitutions set to one half of the sensor response limit (0.0005 ml L^{-1}).

TSM Data Detrending

Biofouling (i.e., the growth of algae and other living materials changing detector sensitivity) was observed for all 32 size classes of TSM. Biofouling resulted in a positive TSM trend between the maintenance events; this trend was described by a logistic curve (Figure 2). The logistic curve corresponds well to the model of biomass growth limited by substrate "carrying capacity", Equation 1, and its solution, Equation 2.

$$\frac{dm}{dt} = rm(1 - \frac{m}{K}), \quad (1)$$

$$m(t) = \frac{K}{1 + Ce^{-r(t-t_0)}} \quad (2)$$

where t was time; ($m = m(t)$) was biomass; r represented growth rate; K represented saturation); and t_0 (the point of inflection) represented positive constant parameters.

To detrend the data, the following procedures were applied. First, the start and end of each period between maintenance events were identified; the end of each period was identified by intervals between observations exceeding one hour (vs. ~six minutes between the observations in normal time-series). Each period was detrended independently for each size class as follows:

1. The time-series in each period between maintenance service was smoothed by calculating the median TSM at 24-hour intervals. The TSM for each of these points in time was estimated as a median of all observations within the 48-hour interval centered around respective points in time.

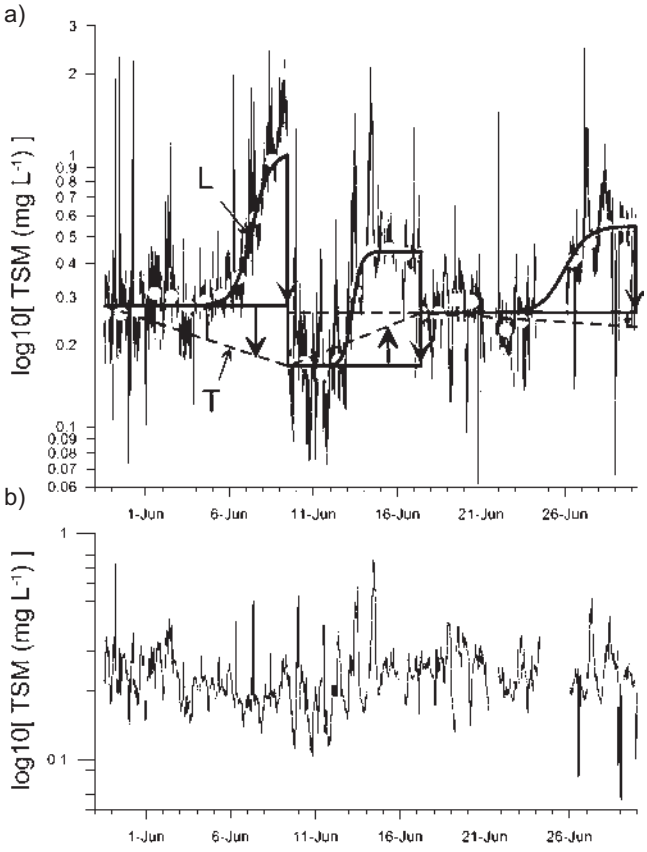

Figure 2. Scheme illustrating the detrending procedure of the TSM concentration of the size class 6.24 µm (LISST-100X channel 6) during the period May 29-June 30 (a). The erroneous increase in TSM induced by biofouling between maintenance events was fitted by logistic curves (L). Differences between TSM measurements before and after each maintenance event were fitted by linear trend (T). Detrended TSM (LISST-100X channel 6; Logged diameter 6.24 µm; b).

2. The parameters of a logistic curve were fitted, in the least squares sense, to this smoothed dataset of 24-hour time intervals. The initial conditions were estimated using the method suggested by Cavallini (1993).

3. Using the parameters (r, K, and t_0), the TSM measurement error (logistic curve) was calculated for each observation and subtracted from the measured TSM data.

4. The linear trend (positive or negative) resulting from differences in detector sensitivity after successive maintenance events was calculated and subtracted from the data (Figure 2).

Principal Component Analysis and Tidal Prism Calculation

The log-transformed, detrended, and normalized (by subtracting the mean from each TSM size class and dividing it by the standard deviation) data matrix was processed using Principal Component Analysis multivariate statistical method (PCA; see Preisendorfer 1988). This method decreases information redundancy by transforming simultaneously measured correlated variables (32 TSM size classes) into a small number of new variables (principal components), where each principal component is a linear combination of the original variables. The coefficients of linear combination are selected in such a way that the variance along the first principal component is the maximum among all possible choices for the first axis. The second principal component is another axis in space, perpendicular to the first; the variance of this variable is the maximum among all possible choices of this second axis. The coefficients of linear combination (factor loadings) show the correlation between the variables; the new variables constructed using these coefficients (factor scores) illustrate the most important independent (uncorrelated) processes of the analyzed system.

The dominating frequencies of variability for the leading PCA modes were identified using the wavelet method (Torrence and Compo 1998). The wavelet transformation takes a one-dimensional function of time and expands it into a two-dimensional function of time and scale. In wavelet representation, a geophysical signal is decomposed into the sum of elementary building blocks describing its local frequency content. The wavelet analysis provides both time and scale information and allows for the separation and sorting of different structures on different time scales at different times. The wavelet transform software for MATLAB was produced by Aslak Grinsted (Jevrejeva *et al*. 2003, Grinsted *et al*. 2004, Moore *et al*. 2005).

The relationship between tides and TSM was analyzed using a modified tidal prism model (e.g., Luketina 1998). For each TSM observation, the effect of tidal flow was estimated from the direction of the tidal flow (flood vs. ebb based on the sign of the first derivative of the tidal depth time-series) and the difference between maximum and minimum tidal levels (tidal prism) during the preceding 6-hour period, which slightly exceeded one-half of the 11.5-hour period dominating tidal cycle. Positive and negative extremes of the resulting variable corresponded to slack water periods. Such extremes were proportional to the volume of water transported through the BCE during the preceding flood (positive extreme) or ebb (negative extreme) tidal phase.

Results

The 3 leading PCA modes described >92% of the TSM variability (Table 1). The first PCA mode (PCA-1) was associated with mid-size particles (7.33 - 237 µm; Figure 3a), the second mode (PCA-2) with small-size class (2.72 - 6.21 µm; Figure 3b), and the third mode (PCA-3) with large-size (280 - 460 µm), and to a lesser degree with small-size particles (Figure 3c).

The mid-size particle class (PCA-1) was likely associated with phytoplankton and the products of its growth (i.e., detritus). The large-scale variations of PCA-1 over time (Figure 4a) were correlated with phytoplankton biomass derived from satellite monitoring (Figure 5c). High concentration of mid-size TSM was observed during the first half of June, gradually decreased from mid-June to mid-July and remained low between late July and August (Figure 4a). In the SMB, high CHL concentration associated with phytoplankton blooms was also observed in the beginning of June (maximum on June 7) and coincided with cold water temperature (Figure 5c) characteristic of an intensive coastal upwelling. During the observed period, upwelling appeared to be a factor regulating phytoplankton growth in the SMB. Short-period drops of water temperature on July 1-2, July 6-7, July 15-17 and near the end of August resulted in small, but significant increases in CHL. However, these small blooms exerted no effect on TSM in the BCE (cf. Figure 4). Temperatures in the SMB and BCE were highly correlated (not shown) indicating intensive water exchange resulting from tidal mixing.

Table 1. Leading PCA modes and associated percent of variability.

PCA Mode	Percent Variability	Accumulated Percent Variability
1	70.92	70.92
2	14.38	85.30
3	7.04	92.34
4	4.47	96.81
5	1.89	98.70

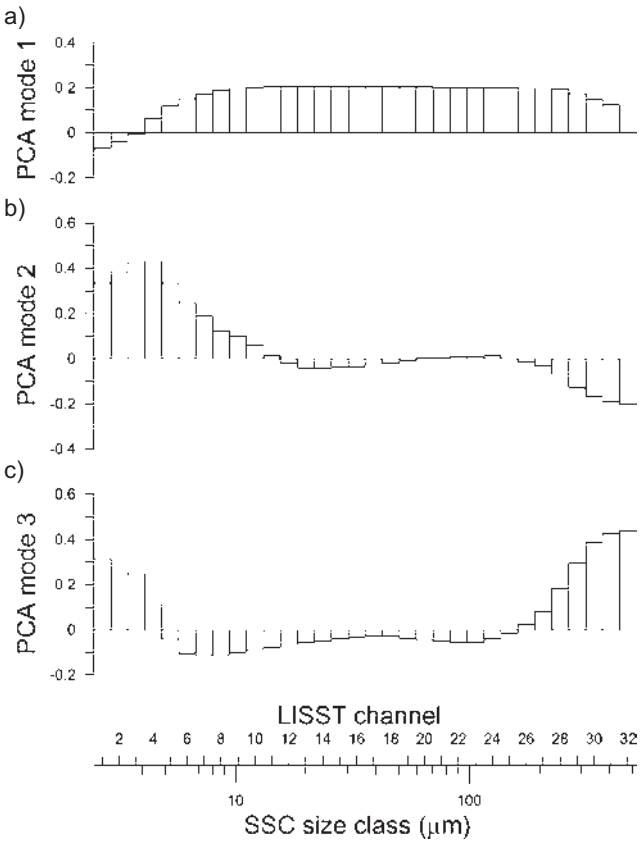

Figure 3. Factor loadings for the three leading PCA modes. PCA-1 is associated with a wide TSM size range (approximately 5 - 300 μm); PCA-2 with small particles (<10 μm) and PCA-3 with large (>200 μm) and partly small (<4 μm) particles.

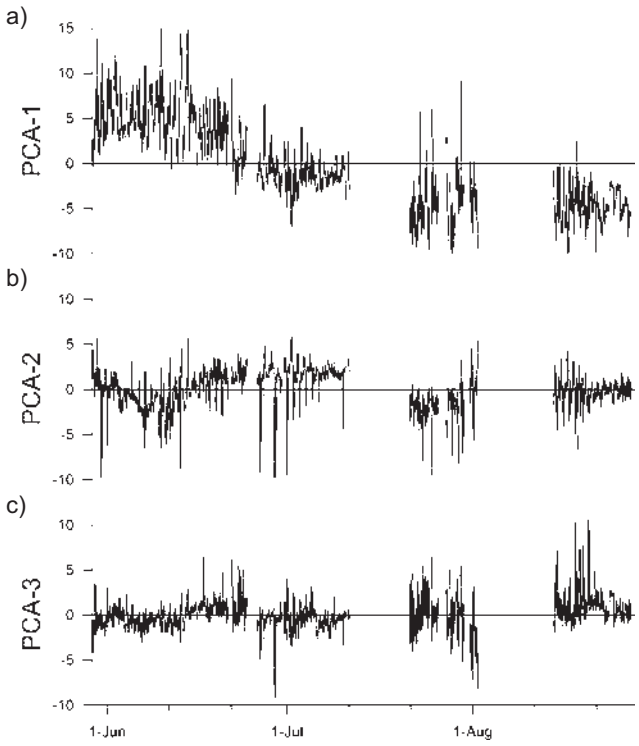

Figure 4. Time-series of the three leading PCA modes.

In spite of the decreasing trend for PCA-1 observed during June-August, wave-driven sediment resuspension could not be assumed as a factor related to the mid-size particle concentration. Wave height in June and the beginning of July was higher than late July-August (Figure 5b), but the decrease observed for PCA-1 (Figure 4a) preceded the decrease in wave height. As such, the role of wave resuspension in TSM dynamics in the BCE appeared to be less significant than the impact of phytoplankton.

Diurnal variability of the mid-sized particles supports the idea that phytoplankton growth (strongly related to diurnal photosynthetic cycle) and/or diel vertical migration played a significant role in formation of these TSM size classes. The wavelet diagram for PCA-1 (mid-sized particles; Figure 6a) illustrates that diurnal variability dominated over other frequencies in June, especially during the neap tide period centered about June 10, when phytoplankton biomass was high and the influence of tidal forcing was small (cf. Figure 5a). Later (July-August), the contribution of semi-diurnal variability to the mid-sized particles variability increased and the contribution of diurnal variations decreased (Figure 6a), representing decreasing role of phytoplankton in TSM.

Small-size particles (PCA-2) did not show an evident trend during the observed period (Figure 4b). Two minima of the PCA-2 (June 7-10 and July 20-22) coincided with neap tides (Figure 5a), indicating the primary role of tides in resuspending small-size particles. Small-sized particle variability was dominated by both diurnal and semi-diurnal frequencies during the entire observed period (Figure 6b).

There was no evident correlation between PCA-3 (large-size particles) and CHL, wave height, and tides (Figure 4c). The variability of this mode was mostly semi-diurnal (Figure 6c) indicating the significant role of tides in resuspension and transport of large-sized particles.

Positive and negative extremes of PCA-2 and PCA-3 coincided with ebb tides (Figure 7), indicating spatial heterogeneity of these TSM size classes within the BCE. As a result of this heterogeneity, the down-estuary tidal flows transported high or low concentrations of these size classes of TSM to the sensor location. Some, but not all, ebb tides were

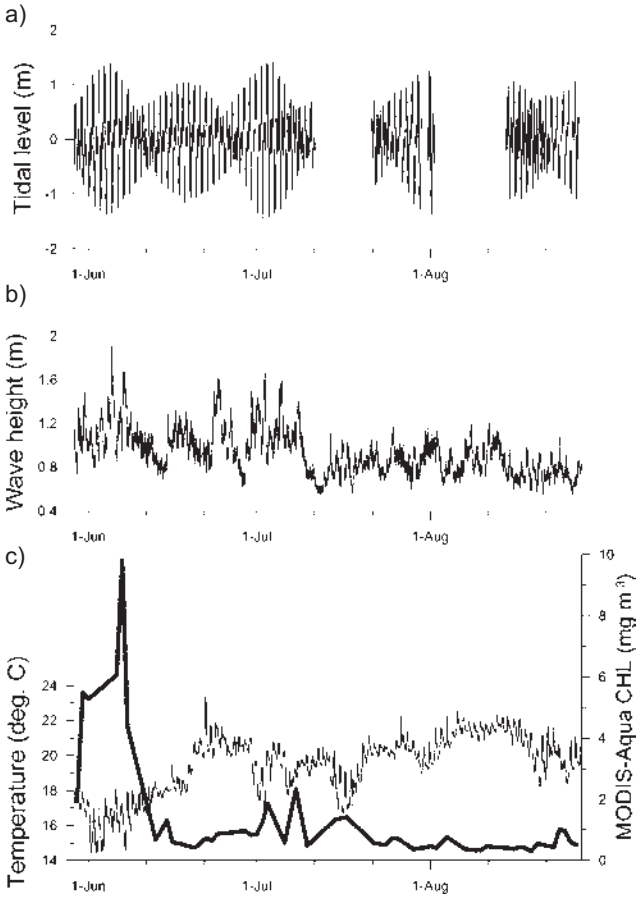

Figure 5. Tidal variability in the Ballona Creek Estuary (a); wave height in the Santa Monica Bay (SMB; b); ocean surface temperature (left Y-axis) and remotely-sensed (MODIS-Aqua) chlorophyll a (CHL) concentration (right Y-axis) in the SMB (c).

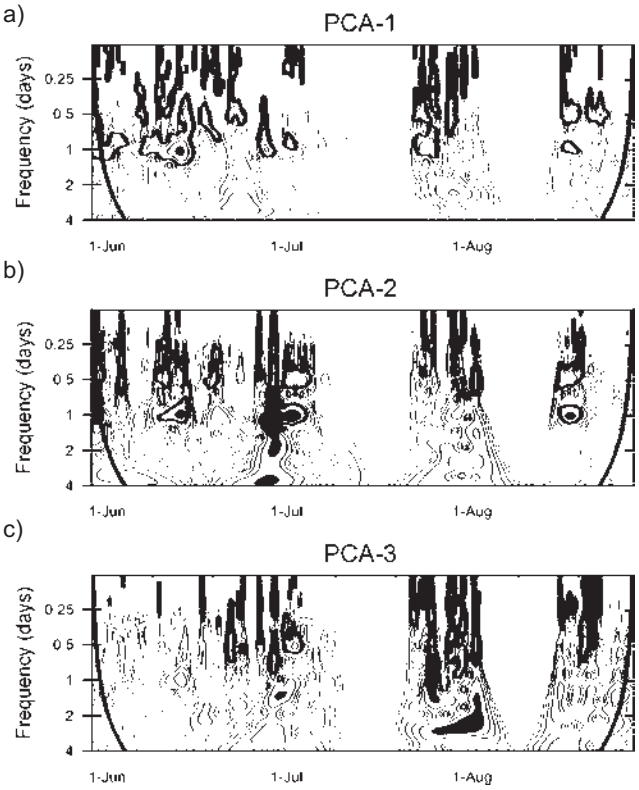

Figure 6. Wavelet diagrams of the time-series of the three leading principle component modes: mid-size particles (PCA-1), small particles (PCA-2), and large-size particles (PCA-3). Absence of variability in mid-July and early August resulted from long periods of maintenance.

associated with PCA-2 decrease and PCA-3 increase (Figure 7). The negative extremes of the tidal prism were characterized by negative PCA-2 and positive PCA-3 (Figure 8), indicating that spring ebb tides transported water with low concentration of small-size particles and high concentration of large-size particles to the BCE mouth area. Extreme flood tides were associated with negative PCA-3 (Figure 8) indicating relatively clean ocean water inflow to the BCE.

Discussion

The deployment of the LISST in the BCE demonstrated that the instrument can provide managers information critical to implementing contaminated sediment management plans. In earlier studies, this instrument was used to study suspended sediment transport in shallow coastal ocean regions driven by wind-induced waves and tidal currents (Ellis *et al*. 2004, Ahn and Grant 2007, Rogers and Ravens 2008, Badewien *et al*. 2009, Bartholoma *et al*. 2009), rivers (Williams *et al*. 2007), and estuaries (Voulgaris and Meyers 2004, Xia *et al*. 2004, Hunt *et al*. 2006).

During deployment, PCA differentiated three different types of particles, and particle movement in the system. The predominant PCA was reflective of biologic particles showing strong correlation with remotely-sensed CHL concentrations and diurnal patterns. Furthermore, particles in the PCA-1 range (7.33 - 237 µm) are typical of diatoms and dinoflagellates (Lalli and Parsons 1997), even taking into account measurement limitations related to the understanding that the LISST was originally designed for sediments and its inversion algorithm assumes that particles are homogeneous spheres with a refraction index typical of inorganic particles (Karp-Boss *et al*. 2007). Similar statistical methodology (PCA) applied earlier to the LISST data collected at two marine bathing beaches in southern

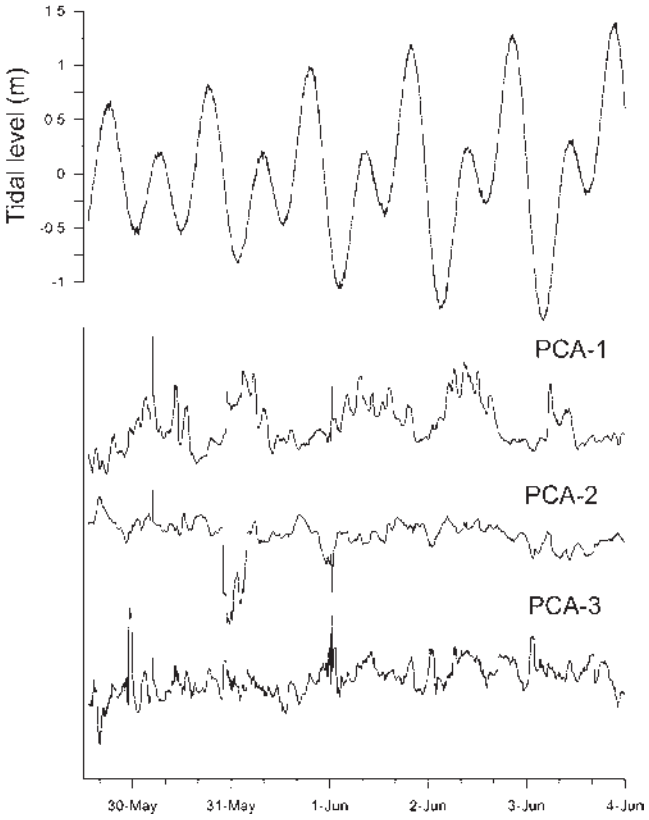

Figure 7. Tidal circulation and the three leading PCA modes representing mid-size particles (PCA-1), small-size particles (PCA-2), and large-size particles (PCA-3).

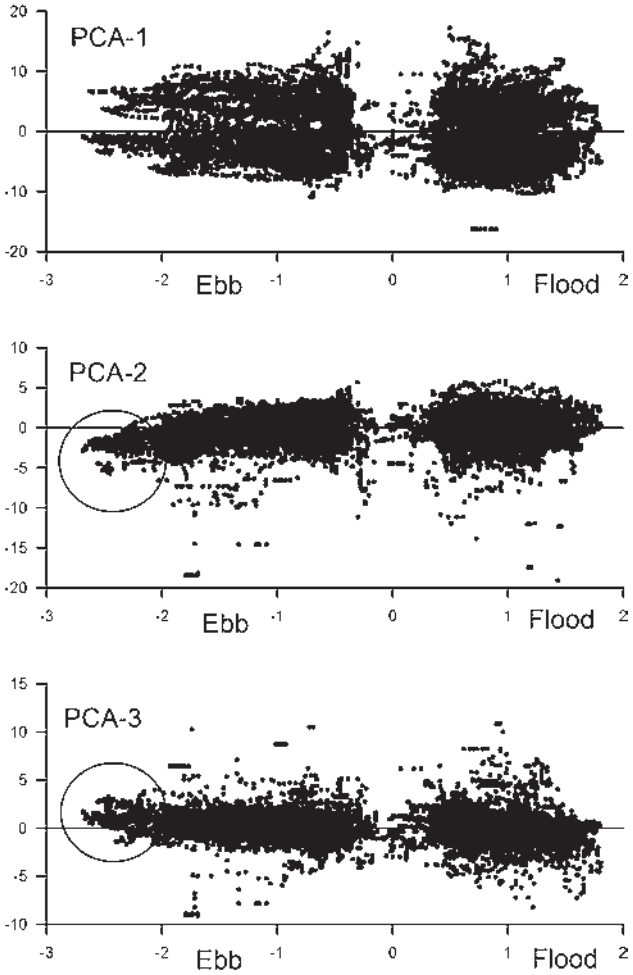

Figure 8. The relationship between tidal circulation (tidal prism defined as the difference between maximum and minimum tidal levels) and the three leading PCA modes. Negative PCA-2 and positive PCA-3 at negative tidal prism extremes are marked with circles.

California (Huntington Beach and Newport Beach) also identified three particle size modes: a phytoplankton (dinoflagellate mode), a large particle mode, and a small particle mode (Ahn and Grant 2007). Diurnal variability of the size class associated with phytoplankton was also documented earlier during LISST observations of coastal bloom and explained by vertical migration (Angles *et al*. 2008).

The small particles (2.72 - 6.21 µm; PCA-2) concentrations were mostly constant throughout the deployment indicating that there was little settling/resuspension. Previous observations in coastal areas dominated by strong tidal circulation revealed a quarter-diurnal cycle related to small particle concentration. This quarter-diurnal cycle was associated with resuspension and settling generated by maximum tidal flow (Ellis *et al*. 2004). A quarter-diurnal cycle was not observed in the BCE, indicating that tidal flows didn't play a significant role in resuspension. At the same time, the lowest small particle concentrations in early June and the end of July were associated with neap tides, when tidal flats in the upper BCE become dry. Fine particles deposited on those flats appear to become depleted during those tides and no source remains in the system, thus fine particle concentrations drop. From this, it is apparent that during the monitoring period shear stresses were not sufficient to significantly mobilize the larger particles.

Larger particles (280 - 460 µm; PCA-3) did not exhibit diurnal patterns, but were correlated with ebb tidal extremes and net export. This agrees with earlier observations indicating that erosion in tidal creeks occurs only during the ebb stage of spring tides, while the tidal creeks do not experience significant erosion during flood tides (Voulgaris and Meyers 2004).

The majority of pollutant loading to the BCE occurs during the wet season, when 90% of the sediments and ~30% of trace metals are discharged from

the watershed and over 50% of the trace metals are particulate bound (Stein and Ackerman 2007). In contrast, during dry periods, the particulate fraction of trace metals is typically less than 10% of the total metals (Stein and Tiefenthaler 2005). Because TSM levels in the BCE did not show a large increase during flood tides, the majority of sediments in the BCE are likely from terrestrial sources. Also, the results of this study indicated that the fine particles in the system become depleted throughout a tidal cycle and only the heavier sands deposited during storms remain. Mitigation of pollutant levels in the BCE could be accomplished by removal of contaminated material via dredging, by controlling watershed sources, or by a combination of the two. The results from the summer monitoring indicate that only modest gains in sediment quality would result in removing contaminated sediments in the BCE. Rather, addressing pollutant sources in the watershed and preventing their introduction into the BCE would produce the greatest improvements in sediment quality because the system is flushed of the typically more contaminated finer particles (SCCWRP, unpublished data).

The methods presented here could be used for biological monitoring, including nutrient control in the watershed. In previous studies, a LISST was used to monitor high-resolution spatio-temporal distribution of coastal phytoplankton blooms including discrimination of phytoplankton at the group and species level (Angles *et al*. 2008, Rienecker *et al*. 2008). In the BCE, a substantial portion of suspended particles was represented by phytoplankton, which do not contribute to sediment contamination but might contribute to eutrophication and hypoxia. Eutrophication, typically resulting from anthropogenic nitrogen discharge (Nixon 1995, Glibert *et al*. 2006), is a growing problem in coastal marine environments (Cloern 2001, Paerl *et al*. 2006). Extremely high phytoplankton biomass in coastal and estuarine environment can adversely affect oxygen balance resulting in hypoxia and anoxia (e.g., Mee 1988). Another adverse effect of coastal eutrophication might be toxins produced by harmful algal species (Paerl 1997, Anderson *et al*. 2002). Because TSM concentrations, specifically those in the phytoplankton size range, are high when CHL blooms are remotely observed in the SMB, it appears that the majority of the CHL in the BCE is associated with offshore phytoplankton and nutrient flux from the sediments in the BCE has minimal impact on their levels.

Literature Cited

Acker, J.G., S. Shen, G. Leptoukh, G. Serafino, G. Feldman and C. McClain. 2002. SeaWiFS ocean color data archive and distribution system: Assessment of system performance. *IEEE Transactions on Geoscience and Remote Sensing* 40:90-103.

Ahn, J.H. and S.B. Grant. 2007. Size distribution, sources, and seasonality of suspended particles in southern California marine bathing waters. *Environmental Science & Technology* 41:695-702.

Anderson, D.M., P.M. Glibert and J.M. Burkholder. 2002. Harmful algal blooms and eutrophication: Nutrient sources, composition, and consequences. *Estuaries* 25:704-726.

Anderson, B., J. Hunt, B. Phillips, B. Thompson, S. Lowe, K. Taberski and R.S. Carr. 2007. Patterns and trends in sediment toxicity in the San Francisco Estuary. *Environmental Research* 105:145-155.

Angles, S., A. Jordi, E. Garces, M. Maso and G. Basterretxea. 2008. High-resolution spatio-temporal distribution of a coastal phytoplankton bloom using laser *in situ* scattering and transmissometry (LISST). *Harmful Algae* 7:808-816.

Ashley, P.M. and M.E. Napier. 2005. Heavy-metal loadings related to urban contamination in the Kooloonbung Creek catchment, Port Macquarie, New South Wales. *Australian Journal of Earth Sciences* 52:843-862.

Badewien, T.H., E. Zimmer, A. Bartholoma and R. Reuter. 2009. Towards continuous long-term measurements of suspended particulate matter (SPM) in turbid coastal waters. *Ocean Dynamics* 59:227-238.

Banse, K. and D.C. English. 1994. Seasonality of Coastal Zone Color Scanner phytoplankton pigment in the offshore oceans. *Journal of Geophysical Research-Oceans* 99:7323-7345.

Bartholoma, A., A. Kubicki, T.H. Badewien and B.W. Flemming. 2009. Suspended sediment transport in the German Wadden Sea-seasonal variations and extreme events. *Ocean Dynamics* 59:213-225.

Bay, S.M., K.C. Schiff, D. Greenstein and L.L. Tiefenthaler. 1998. Stormwater runoff effects on Santa Monica Bay, toxicity, sediment quality, and benthic community impacts. pp. 900-921 *in*: O. T.

Magoon , H. Converse, B. Baird and M. Miller-Henson (eds.), California and the World Ocean '97. American Society of Civil Engineers. Reston, VA.

Bollmohr, S., P.J. van den Brink, P.W. Wade, J.A. Day and R. Schulz. 2009. Spatial and temporal variability in particle-bound pesticide exposure and their effects on benthic community structure in a temporarily open estuary. *Estuarine Coastal and Shelf Science* 82:50-60.

Buffleben, M.S., K. Zayeed, D. Kinmbrough, M.K. Stenstrom and I.H. Suffet. 2002. Evaluation of urban non-point source runoff of hazardous metals entering Santa Monica Bay, California. *Water Science and Technology* 45:263-268.

Campbell, J.W. 1995. The lognormal-distribution as a model for biooptical variability in the sea. *Journal of Geophysical Research-Oceans* 100:13237-13254.

Cavallini, F. 1993. Fitting a logistic curve to data. *The College Mathematics Journal* 24:247-253.

Cloern, J.E. 2001. Our evolving conceptual model of the coastal eutrophication problem. *Marine Ecology - Progress Series* 210:223-253.

Ellis, K.M., D.G. Bowers and S.E. Jones. 2004. A study of the temporal variability in particle size in a high-energy regime. *Estuarine Coastal and Shelf Science* 61:311-315.

Fairey, R., C. Roberts, M. Jacobi, S. Lamerdin, R. Clark, J. Downing, E. Long, J. Hunt, B. Anderson, J. Newman, R. Tjeerdema, M. Stephenson and C. Wilson. 1998. Assessment of sediment toxicity and chemical concentrations in the San Diego Bay region, California, USA. *Environmental Toxicology and Chemistry* 17:1570-1581.

Foster, G.D. and V. Cui. 2008. PAHs and PCBs deposited in surficial sediments along a rural to urban transect in a Mid-Atlantic coastal river basin (USA). *Journal of Environmental Science and Health Part a-Toxic/Hazardous Substances & Environmental Engineering* 43:1333-1345.

Gartner, J.W., R.T. Cheng, P.F. Wang and K. Richter. 2001. Laboratory and field evaluations of the LISST-100 instrument for suspended particle size determinations. *Marine Geology* 175:199-219.

Glibert, P.M., J. Harrison, C. Heil and S. Seitzinger. 2006. Escalating worldwide use of urea - a global change contributing to coastal eutrophication. *Biogeochemistry* 77:441-463.

Grinsted, A., J.C. Moore and S. Jevrejeva. 2004. Application of the cross wavelet transform and wavelet coherence to geophysical time series. *Nonlinear Processes in Geophysics* 11:561-566.

Hipsey, M.R., J.D. Brookes, R.H. Regel, J.P. Antenucci and M.D. Burch. 2006. In situ evidence for the association of total coliforms and *Escherichia coli* with suspended inorganic particles in an Australian reservoir. *Water Air and Soil Pollution* 170:191-209.

Hornberger, M.I., S.N. Luoma, A. van Geen, C. Fuller and R. Anima. 1999. Historical trends of metals in the sediments of San Francisco Bay, California. *Marine Chemistry* 64:39-55.

Hunt, S., C.J. Lemckert and C. Schacht. 2006. Location of turbidity maxima within a microtidal estuary and some limitations of laser *in situ* particle sizing. *Journal of Coastal Research* 1:520-525.

Jevrejeva, S., J.C. Moore and A. Grinsted. 2003. Influence of the Arctic Oscillation and El-Nino-Southern Oscillation (ENSO) on ice conditions in the Baltic Sea: The wavelet approach. *Journal of Geophysical Research-Atmospheres* 108:4677.

Karp-Boss, L., L. Azevedo and E. Boss. 2007. LISST-100 measurements of phytoplankton size distribution: evaluation of the effects of cell shape. *Limnology and Oceanography-Methods* 5:396-406.

Lalli, C.M. and T.R. Parsons. 1997. Biological oceanography : An introduction (2nd edition). Butterworth Heinemann. Oxford, UK.

Liu, D.F., J.J. Sansalone and F.K. Cartledge. 2004. Adsorption characteristics of oxide coated buoyant media (rho(s) <1.0) for storm water treatment. *Journal of Environmental Engineering-ASCE* 130:374-382.

Luketina, D. 1998. Simple tidal prism models revisited. *Estuarine, Coastal and Shelf Science* 46:77-84.

Mee, L.D. 1988. A definition of "critical eutrophication" in the marine environment. *Revista de Biologia Tropical* 36:159-161.

Meral, R. 2008. Laboratory evaluation of acoustic backscatter and LISST methods for measurements of suspended sediments. *Sensors* 8:979-993.

Mikkelsen, O.A. and M. Pejrup. 2001. The use of a LISST-100 laser particle sizer for in-situ estimates of flee size, density and settling velocity. *Geo-Marine Letters* 20:187-195.

Moore, J.C., A. Grinsted and S. Jevrejeva. 2005. New tools for analyzing time series relationships and trends. *EOS* 86:226,232.

Mucha, A.P., M. Vasconcelos and A.A. Bordalo. 2003. Macrobenthic community in the Douro estuary: relations with trace metals and natural sediment characteristics. *Environmental Pollution* 121:169-180.

Nixon, S.W. 1995. Coastal marine eutrophication: A definition, social causes, and future concerns. *Ophelia* 41:199-219.

O'Day, P.A., S.A. Carroll, S. Randall, R.E. Martinelli, S.L. Anderson, J. Jelinski and J.P. Knezovich. 2000. Metal speciation and bioavailability in contaminated estuary sediments, Alameda Naval Air Station, California. *Environmental Science & Technology* 34:3665-3673.

O'Reilly, J.E., S. Maritorena, B.G. Mitchell, D.A. Siegel, K.L. Carder, S.A. Garver, M. Kahru and C. McClain. 1998. Ocean color chlorophyll algorithms for SeaWiFS. *Journal of Geophysical Research-Oceans* 103:24937-24953.

Paerl, H.W. 1997. Coastal eutrophication and harmful algal blooms: Importance of atmospheric deposition and groundwater as "new" nitrogen and other nutrient sources. *Limnology and Oceanography* 42:1154-1165.

Paerl, H.W., L.M. Valdes, B.L. Peierls, J.E. Adolf and L.W. Harding, Jr. 2006. Anthropogenic and climatic influences on the eutrophication of large estuarine ecosystems. *Limnology and Oceanography* 51:448-462.

Preisendorfer, R.W. 1988. Principal component analysis in meteorology and oceanography. Elsevier Science. New York, NY.

Rate, A.W., A.E. Robertson and A.T. Borg. 2000. Distribution of heavy metals in near-shore sediments of the Swan River estuary, Western Australia. *Water Air and Soil Pollution* 124:155-168.

Rienecker, E.V., J.P. Ryan, M. Blum, C. Dietz, L. Coletti, R. Marin, III and W.P. Bissett. 2008. Mapping phytoplankton *in situ* using a laser-scattering sensor. *Limnology and Oceanography-Methods* 6:153-161.

Rogers, A.L. and T.M. Ravens. 2008. Measurement of longshore sediment transport rates in the surf zone on Galveston Island, Texas. *Journal of Coastal Research* 24:62-73.

Sabin, L.D., K.A. Maruya, W. Lao, D.W. Diehl, D. Tsukada, K.D. Stolzenbach and K.C. Schiff. 2008. Exchange of polycyclic aromatic hydrocarbons between the atmosphere, water, and sediment in southern California coastal embayments. pp. 51-64 *in*: S.B. Weisberg and K. Miller (eds.), Southern California Coastal Water Research Project 2008 Annual Report. Costa Mesa, CA.

Sequoia Scientific. 2007. LISST-100X Particle Size Analyzer, User's Manual Version 4.65. Bellevue, WA.

Serra, T., J. Colomer, X.P. Cristina, X. Vila, J.B. Arellano and X. Casamitjana. 2001. Evaluation of laser *in situ* scattering instrument for measuring concentration of phytoplankton, purple sulfur bacteria, and suspended inorganic sediments in lakes. *Journal of Environmental Engineering-ASCE* 127:1023-1030.

Slade, W.H. and E.S. Boss. 2006. Calibrated near-forward volume scattering function obtained from the LISST particle sizer. *Optics Express* 14:3602-3615.

Stein, E.D. and D. Ackerman. 2007. Dry weather water quality loadings in arid, urban watersheds of the Los Angeles Basin, California, USA. *Journal of American Water Resource Association* 43:398-413.

Stein, E.D. and L. Tiefenthaler. 2005. Dry-weather metals and bacteria loading in an arid, urban watershed: Ballona Creek, California. *Water, Air, and Soil Pollution* 164:367-382.

Styles, R. 2006. Laboratory evaluation of the LISST in a stratified fluid. *Marine Geology* 227:151-162.

Torrence, C. and G.P. Compo. 1998. A practical guide to wavelet analysis. *Bulletin of the American Meteorological Society* 79:61-78.

Traykovski, P., R.J. Latter and J.D. Irish. 1999. A laboratory evaluation of the laser *in situ* scattering

and transmissometery instrument using natural sediments. *Marine Geology* 159:355-367.

Ujevic, I., N. Odzak and A. Baric. 2000. Trace metal accumulation in different grain size fractions of the sediments from a semi-enclosed bay heavily contaminated by urban and industrial wastewaters. *Water Research* 34:3055-3061.

Voulgaris, G. and S.T. Meyers. 2004. Temporal variability of hydrodynamics, sediment concentration and sediment settling velocity in a tidal creek. *Continental Shelf Research* 24:1659-1683.

Williams, N.D., D.E. Walling and G.J.L. Leeks. 2007. High temporal resolution *in situ* measurement of the effective particle size characteristics of fluvial suspended sediment. *Water Research* 41:1081-1093.

Xia, X.M., Y. Li, H. Yang, C.Y. Wu, T.H. Sing and H.K. Pong. 2004. Observations on the size and settling velocity distributions of suspended sediment in the Pearl River Estuary, China. *Continental Shelf Research* 24:1809-1826.

Acknowledgements

The authors would like to thank the City of Los Angeles for partial funding of this effort. The authors also thank Jeff Brown and Eric Stein for providing help with deployment, servicing, study design, and review of early manuscript drafts.